



Estimation of Laminar-to-Turbulent Transition Using Empirical and Numerical Methods for Various Aerodynamic Forms

Nina V. Voevodenko¹, Anatoly A. Gubanov¹, Dmitry S. Ivanyushkin¹, Yury G. Shvaley¹

Abstract

This paper presents the results of methodological studies aimed at investigating the ability to determine the position of the laminar-to-turbulent transition (LTT) using empirical criteria and numerical methods. The criteria of Simeonides and Berry have been investigated, and their results are compared with the experimental data and with the results of the numerical solution of the RANS equations with the transition turbulence model. Methodical studies were carried out for a flat plate, and for cones with different angles at the apex at zero and nonzero angles of attack. The studies were carried out in the range of Mach numbers $M = 2 \div 10$ and Reynolds numbers $Re = (3 \div 45) \cdot 10^6$. Also, different methods for determining LTT on a complex surface of the HEXAFly-INT glider model were compared.

Keywords : *laminar-to-turbulent transition, CFD simulation, empirical criteria, experiment*

Nomenclature

¹Central Aerohydrodynamic Institute named after Professor N.E. Zhukovsky (TsAGI), 1, Zhukovsky str., Zhukovsky Moscow region, 140180, Russia, nina.voevodenko@tsagi.ru

Latin

LTT – Laminar-to-turbulent transition
 BL – Boundary layer
 RANS – Reynolds Averaged Navier-Stokes equations
 M – Mach number
 Re – Reynolds number
 St – Stanton number
 AoA – Angle of Attack
 TET - half-angle at the cone vertex
 C_f – Friction drag coefficient
 p – flow pressure
 u, v, w – flow velocity components
 T – temperature
 r – coefficient of recovery of the flow temperature
 Re_{trans} – Reynolds number of LTT beginning

$Re_{\Delta x}$ – LTT length in Reynolds number
 Re_b – Reynolds number based on the leading bluntness radius
 Re_θ - Reynolds number based on the boundary layer momentum thickness

Greek

α – Angle of Attack
 ρ – flow density
 μ – dynamic viscosity coefficient
 θ - half-angle at the cone vertex

Subscripts

e – parameter on the external boundary of BL
 ∞ - parameter in the free stream
 w – parameter on the wall
 r – recovery parameter

Introduction

At high supersonic flight speeds, the LTT is one of the most important physical phenomena which influence on the vehicle aerodynamics. LTT affects substantially on the thermal processes, on the drag coefficient and on the vehicle Lift-to-Drag ratio. Numerical simulation of LTT is a very difficult task even for the modern level of development of computer technology and numerical methods. A correct numerical simulation of LTT is possible on the basis of direct numerical simulation of the Navier-Stokes equations solution (DNS methods). However, even supercomputers now allow simulating the three-dimensional non-stationary DNS solutions only for fairly simple geometries, such as a plate or ramp. Building a DNS solution for a complex geometry close to the forms of real aircraft is technically impossible because it requires computational volumes and computer resources that do not exist in principle.

In connection with the complexity of the phenomenon under consideration, along with numerical simulation, empirical methods are developed that predict the beginning of LTT and its extent with the help of simple formulas obtained as a result of generalization and analysis of large arrays of experimental data obtained both in wind tunnels and in flight experiments. However, empirical methods also have significant limitations in terms of the range of application and accuracy.

Therefore, a complex approach was used in this work to study LTT using various methods: 1) Determining the beginning and length of LTT zone using empirical formulas and criteria; 2) Experimental studies of LTT in TsAGI's wind tunnel (WT) T-116; 3) Numerical modelling of LTT using CFD methods based on solving the Reynolds Averaged Navier-Stokes (RANS) equations.

1. Empirical criteria and its implementation in numerical tool

As noted above, modern high-level numerical methods and computer capabilities do not allow the simulation of the flows with a laminar-turbulent transition on complex-shaped surfaces correctly and reliably. Therefore, a numerical method based on empirical criteria for the beginning and extension of LTT was developed to predict LTT on the surfaces of aircraft close to real ones. The basis of this method of numerical modeling of high-speed flow around bodies is the numerical solution of the Euler equations using the Hypersonic small disturbance theory and Godunov-Kolgan numerical method. This methodology is realized in the program package NINA, which was developed earlier in TsAGI and is described in detail in [1-2]. As a result of the Euler equations numerical solution, we obtain the parameters of the inviscid flow on the body surface and then use them as parameters at the external boundary of the boundary layer (BL). The numerical solution of the equations of inviscid gas flow can be obtained with the help of any other package that realizes a numerical solution of the Euler equations. In principle, a numerical solution of the averaged Navier-Stokes equations (RANS) can be used for this, but the use of the solution of the Euler equations in

this case is more rigorous and correct. In addition, in the case of using the RANS equations solution, the question arises which cells are considered as external with respect to the BL, where large parameter gradients arise. This leads to ambiguous solution when using RANS solutions, so the use of the Euler's equations solutions in this case is more correct and preferable.

Thus, the algorithm for constructing a numerical solution is as follows:

1. As a result of the numerical solution of the Euler equations (NINA package), we obtain the values of the parameters of the inviscid flow in the center of the cell adjacent to the surface of the body. We accept the values of the parameters in the cells adjoining to the surface of the body for the values of the parameters at the outer boundary of the boundary layer (BL). We obtain the following local parameters in the cell at the external boundary of BL: pressure - p_e , density - ρ_e , velocity components - u_e, v_e, w_e .
2. From the parameters obtained on the outer BL boundary, we calculate the local Mach number - M_e and the local Reynolds number - Re_e .
3. We calculate the local Stanton number - St and the local friction coefficient - C_f using the empirical formulas given below, Eq. 1 - 4. To calculate St and C_f we also need the wall temperature T_w . The temperature of the free stream - T_∞ and T_w are given, if they are known, or also determined by some empirical technique.
4. Using empirical criteria, we determine the critical Reynolds number - Re_{trans} of the LTT beginning and its length - $Re_{\Delta x}$.
5. By comparing the local Reynolds number - Re_e and the numbers Re_{trans} and $Re_{\Delta x}$, we determine whether the flow at a given point is laminar, turbulent or transient. Depending on this, we choose the values of St and C_f .

To calculate the local Stanton number - St_e number and the friction drag coefficient - C_{fe} for a laminar and turbulent BL, we use the empirical formulas of Yu.G. Shvalev and N.F. Ragulin [3-4]. These formulas were obtained on the basis of numerous experimental studies in the TsAGI's wind tunnel T-116:

$$St_e|_{lam} = 0.415 \cdot Re_e^{-0.5} (1 + 0.2rM_e^2)^{-0.116} (T_w/T_r)^{-0.116}, T_r = T_e(1 + 0.168M_e^2), r = 0.86 \quad (1)$$

$$St_e|_{turb} = 0.028 \cdot Re_e^{-0.18} (1 + 0.2rM_e^2)^{-0.47} (T_w/T_r)^{-0.24}, T_r = T_e(1 + 0.178M_e^2), r = 0.89 \quad (2)$$

$$St_e = \frac{\alpha_e}{\rho_e v_e c_e}, \quad Re_e = \frac{\rho_e v_e x}{\mu_e}, \quad \rho_e v_e = 0.0697 \frac{P_e M_e}{\sqrt{T_e}}$$

r is the coefficient of recovery of the flow temperature.

The Reynolds analogy on the relationship between friction and heat transfer makes it possible to obtain an equation for determining local coefficients of friction. This relationship is determined by the relation:

$$c_f = 2S \cdot St_e,$$

$S = 0.825$ in the turbulent BL and $S = 0.8$ in the laminar BL.

Consequently, we obtain the following empirical formulas for calculating the local friction coefficients:

$$c_{fe}|_{lam} = 0.664 \cdot Re_e^{-0.5} (1 + 0.2rM_e^2)^{-0.116} (T_w/T_r)^{-0.116}, \quad (3)$$

$$c_{fe}|_{turb} = 0.0462 \cdot Re_e^{-0.18} (1 + 0.2rM_e^2)^{-0.47} (T_w/T_r)^{-0.24} \quad (4)$$

If the local Reynolds number $Re_e < Re_{trans}$, we take the values of the local Stanton number and the friction coefficient equal to the corresponding values for the laminar BL, Eq. 1 and 3, if $Re_e > Re_{trans} + Re_{\Delta x}$, we take the values of the local Stanton number and the friction coefficient equal to the corresponding values for the turbulent BL, Eq. 2 and 4, if $Re_{trans} < Re_e < Re_{trans} + Re_{\Delta x}$, the local Stanton number and the friction coefficient are determined by linear approximation.

To determine the values of Re_{trans} and $Re_{\Delta x}$, various empirical criteria can be used. In this paper, two criteria were chosen as the empirical criteria for studying: Simeonides [5] and Berry [6], which were obtained on the basis of processing large arrays of various experimental data and are quite simple. Simeonides criterion [5] for a plate with a large blunt radius of the leading edge:

$$Re_{trans} = 6 \cdot 10^6 \cdot M_e^{1.38} \cdot Re_b^{-0.19}, \quad (5)$$

and for the cone:

$$Re_{trans} = 5 \cdot 10^5 \cdot M_e^{0.80} \cdot Re_b^{0.1}, \quad (6)$$

where M_e is the Mach number at the outer boundary of the boundary layer, Re_b is the Reynolds number calculated from the doubled radius of blunting. The length of the transition zone was calculated using the formula:

$$Re_{\Delta x} = (60 + 4.86 \cdot M_e^{1.92}) \cdot Re_{trans}^{2/3}. \quad (7)$$

According to the Simeonides criterion, the main parameters determining LTT are the Mach number and the blunt radius of the leading edge of the body.

The second criterion considered in this paper is the Berry criterion [6]:

$$Re_{\theta}/M_e \geq 300 \div 450 \quad (8)$$

The Reynolds number of the LTT is determined by the Reynolds number based on the boundary layer momentum thickness Re_{θ} .

2. CFD simulation

For the numerical simulation of the flow around configurations, ANSYS FLUENT software package was used. Numerical simulations were performed on the basis of the RANS solutions. For LTT modelling, the SST $\gamma - Re_{\theta}$ Lentry-Menter model of turbulence (Langtry & Menter SST-Transition Model) was used, in which the LTT position is determined automatically based on the Local Correlation-based Transition Modeling (LCTM) concept. The approach described above is not completely correct for supersonic flows, since the Lentry-Menter model was developed for subsonic flows. Therefore, in order to improve the reliability of the results, along with the CFD methods, the LTT empirical criteria are applied.

ANSYS FLUENT implements two models of turbulence with the possibility of modeling a laminar-turbulent transition: k-kl-w and Transition SST (better known as $\gamma - Re_{\theta}$ or Lentry-Menter model). In the present paper, the SST $\gamma - Re_{\theta}$ model [7] was chosen for numerical modeling of flows with LTT based on the transport equation for the intermittency factor γ , since it is the most universal and is intended for describing all types of transition.

Calculation of complex aerodynamic configuration requires the use of grids of large dimension. The calculation grid is formed in three stages. At the first stage, a non-structured triangular grid was built on the surface of the model, and it was checked for errors and elements with poor quality. If necessary, adaptation of the surface mesh for a more accurate description of the elements of the model was carried out. At the second stage, to compute the flow in the boundary layer on the surface grid, a layer of prismatic elements was built up (the height of the first layer of prisms corresponded to the value $Y^+ = 1$), after which the grid was re-aligned. At the final stage, the inner volume of the computational domain was filled with tetrahedral cells with a build-up coefficient of 1.2. In the following examples of calculations, the dimension of the computed grid was about 20,000 00 cells for the semi-model. An example of a computational grid is shown in Fig. 1. The size of the calculated region was chosen from the condition that the external boundaries on which the conditions of the unperturbed flow were set were not influenced. On a hard surface, adhesion conditions were fulfilled. To achieve convergence and obtain a steady-state stationary solution, an average of 10,000 to 15,000 iterations was required.

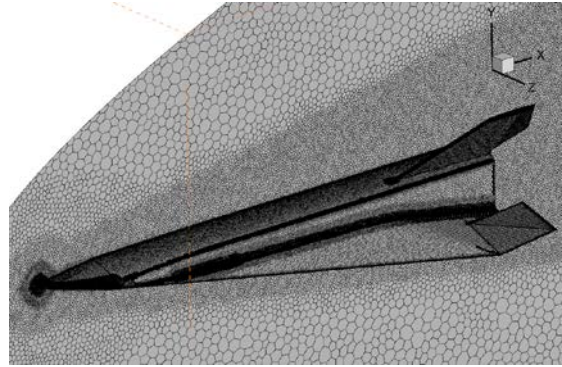


Fig 1. Example of numerical grid for ANSYS FLUENT.

3. Experimental studies

To validate the computational methods and determine the range of their applicability, the numerical and experimental data were compared. Experimental data were obtained in the WT T-116 of TsAGI. The region of transition to the model surface was determined by the thermal method according to the values of the heat transfer coefficient (the Stanton number) which was determined by means of special temperature sensors. The determination of the transition region is based on a significant difference of the Stanton numbers in the laminar and turbulent boundary layers [3, 4].

The studies were carried out in the range of Mach numbers $M = 2 \div 10$ and Reynolds numbers $Re = (3 \div 45) \cdot 10^6$, both for simple geometric shapes (plate and cone) and for the complex configuration of the glider HEXAFLY-INT. The data of LTT studies on the HEXAFLY-INT model are described in detail in [5]. The HEXAFLY-INT model installed in the T-116 test section is shown on Fig. 2.

The T-116 wind tunnel (WT) have the squared test section of $2.35\text{m} \times 1\text{m} \times 1\text{m}$ size and allows to carry out a wide variety of aerodynamic research of the aircraft models and of their components at super- and hypersonic flow velocities. The Mach number in the WT tests section varies from $M=1.8$ up to $M=10$. The unit Reynolds number Re variation range (referred to model length of 1m) is from $2.5 \cdot 10^6$ up to $42 \cdot 10^6$. These data correspond to modeled full-scale Re -numbers for 15 – 40 km height for flying vehicles (for characteristic vehicle length $L=6$ m). The T-116 Test Facility is a blow-down WT of ejector type with exhaust into atmosphere, with a variable supersonic diffuser and three-staged ejector. The tunnel is powered by pressure tank; the air is exhausted into atmosphere. The WT is equipped with electric heaters in order to prevent the air condensation in the test section.



Fig. 2 HEXAFLY-INT EFTV wind tunnel model and T-116 wind tunnel at TsAGI.

T-116 is a unique facility, it is super- and hypersonic WT of continuously working regime (test duration up to 7 minutes). It makes possible to obtain the steady-state flow pattern, and so, the results obtained correspond to the flight conditions more adequately, than those obtained in short-run

WTs. This enables more proper link between wind tunnel and flight experiments and improves the understanding of the relevant flow physics and to further validate and improve the applied CFD tools.

Laminar-to-turbulent boundary layer transition on the model surface was investigated using the so called 'regular heating regime method'. The method is based on significant difference between the local heat transfer coefficients on the model surface corresponding to laminar and turbulent boundary layers. Local heat transfer coefficients are determined measuring the rate of temperature change on specially prepared elements of the model surface during the wind-tunnel tests. The method was developed by G.M. Kondratiev [9] and further modifications were elaborated in several subsequent scientific works.

The local flow parameters outside of the boundary layer on the wind- and leeside of the model used for calculations of local heat transfer coefficients, were determined approximately using relations for the oblique shock-waves and Prandtl–Meyer expansion flows, using the local angles of inclination of the model surface to the free-stream flow. The Stanton number obtained as a result of the experimental measurements is compared with the reference values for laminar and turbulent PS, namely with the values obtained from formulas (1) and (2) for laminar and turbulent PS, respectively.

To investigate LTT it is necessary to manufacture a special model for the T-116 wind tunnel with special sensors. In experimental studies, the local values of the heat transfer coefficient are determined by measuring the rate of change in surface temperature by means of special thermocouples whose location on the surface of the model is shown in Fig. 3. Comparison with the reference values of the Stanton number allows one to determine whether the current is laminar, turbulent or transient at a given point.

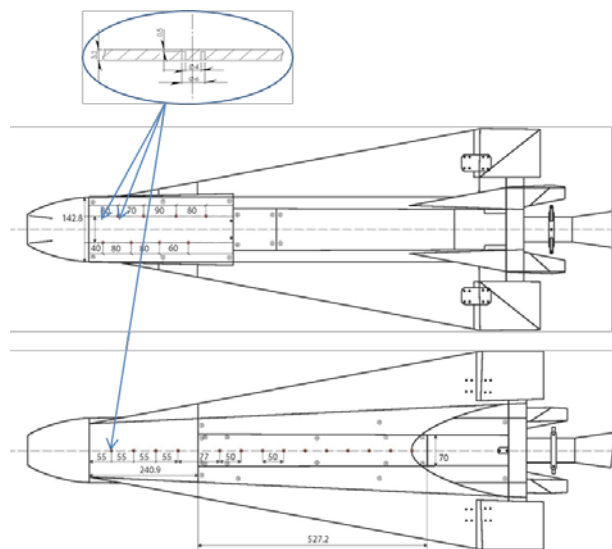


Fig. 3 Location of thermocouples on leeward (top) and windward side (bottom) of the model.

4. Results comparison and analysis

In the wind tunnel TsAGI T-116 at various times, experimental studies of LTT were carried out on different models. Experimental data cover a wide range of Mach and Reynolds numbers: $M = 1.8 \div 10$, $Re_{1M} = 3 \cdot 10^6 \div 45 \cdot 10^6$. The results obtained for the rectangular wing and cone models are presented in paper [10].

The rectangular wing model had a 5% profile and a chord of 800 mm. The upper working surface of the model was carefully polished, and the leading edge had a blunting radius of 0.5 mm. Fig. 4 shows the change in the Stanton number along the flow along the surface of a rectangular wing. Here, a comparison of the experimental results and calculations of LTT with the empirical criteria of Simeonides and Berry is shown.

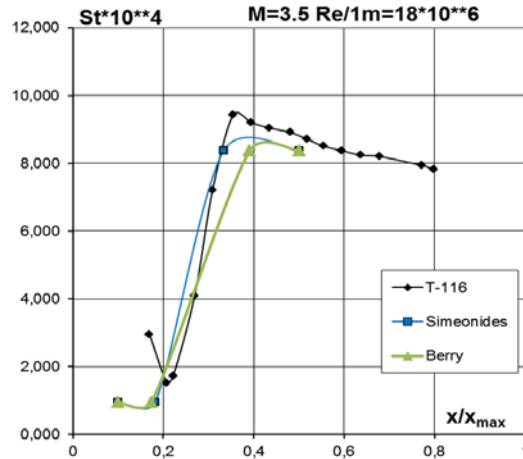


Fig. 4 LTT on the plate surface – comparison of the experimental results and the empirical criteria data.

On the rectangular wing, the Berry criterion, Eq. 8, gave results very close to the experimental data obtained in T-116. Criterion of Simeonides in the original form, Eq. 5, gave results with a much later LTT than in T-116, so it was modified.

The results of studies of the Reynolds number of the beginning and the end of the Re_{tr} transition region on the rectangular wing model in the range of numbers $M=1.8 \div 4$, $Re_{1m} = 5 \cdot 10^6 \div 45 \cdot 10^6$ are shown in Fig. 5, which shows the curves of the beginning and end of the LTT on the rectangular wing as a function of the Mach number. Empirical formulas give quite good results.

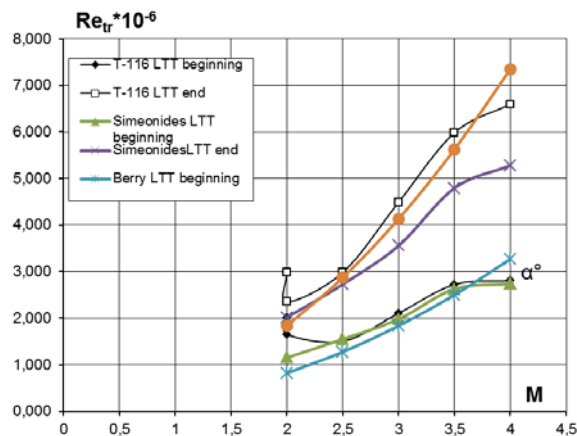


Fig. 5 LTT on the plate surface – comparison of the experimental results and the empirical criteria data.

At the next step, LTT studies were carried out on the surface of the cones. The results of LTT studies on models of cones with a half-angle at the vertex $\theta = 5^\circ, 10^\circ$ and 20° are presented in paper [10]. The studies were carried out at flow velocities corresponding to the numbers $M = 3, 3.5, 4, 7$ and 10 , with Reynolds numbers per 1m $Re_{1m} = 3 \cdot 10^6 \div 35 \cdot 10^6$, in the range of angles of attack (AoA) $\alpha = 0 \div 30^\circ$. LTT studies on the cone surface for the same regimes were also performed using a numerical method with empirical criteria. Fig. 6 and 7 show the results of calculating of the beginning and the end of the LTT on the surface of the cone with a half-angle at the apex of 10° and 20° for $\alpha = 0$ and $M = 3, 3.5, 4$. The beginning and end of the LTT were determined using the Simeonides and Berry formulas for the cone. The beginning of the transition, obtained in the experiment in T-116, is shown by a black line with dots. As can be seen from the presented graphs, the beginning of the LTT, defined by the Simeonides criterion in this case is much closer to the experimental data than by the Berry criterion. The length of the transition zone, calculated by different criteria is very different.

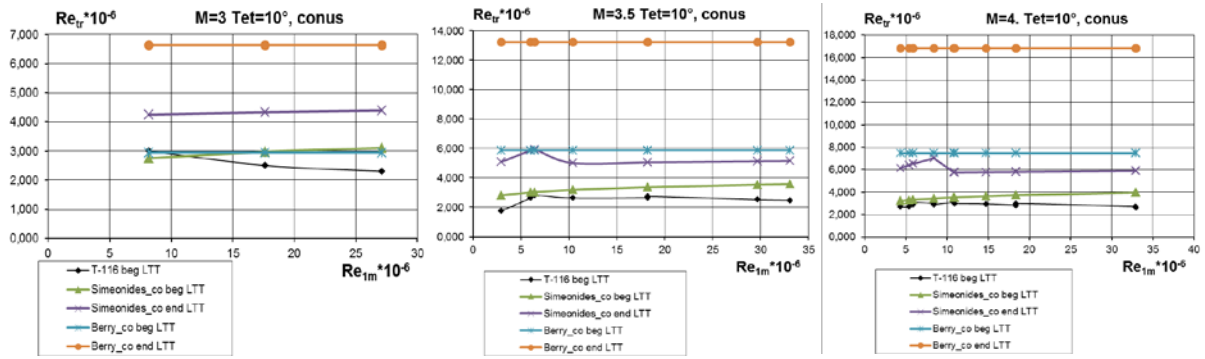


Fig. 6 LTT on the cone surface – comparison of the experimental results and the empirical criteria data.

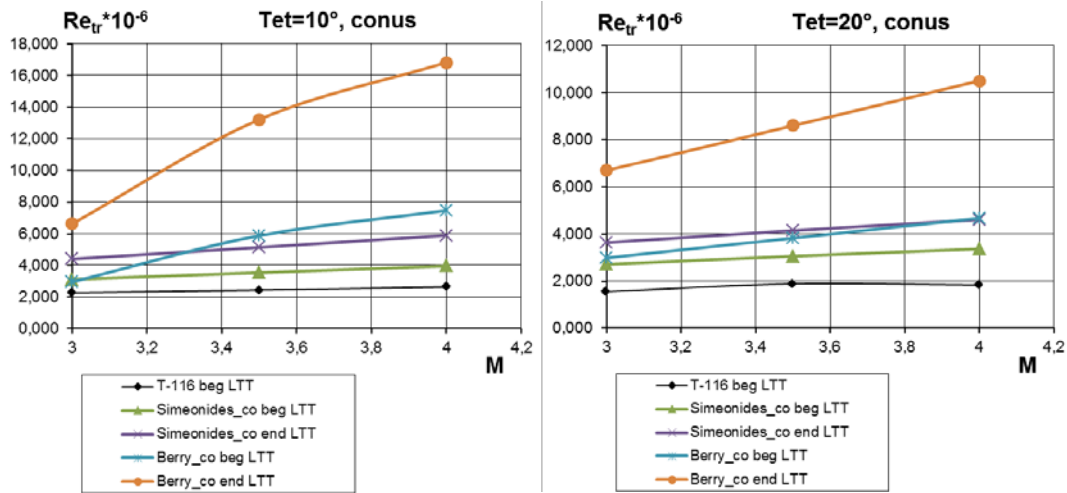


Fig. 7 LTT on the cone surface – comparison of the experimental results and the empirical criteria data.

The distribution of the Stanton number on the cone surface with $\theta = 10^\circ$ at $M = 7$ and $\alpha = 20^\circ$, obtained using a numerical method with the Simeonides criterion is shown in Fig. 8. The right side of this figure shows a comparison of the distribution of the Stanton number along the lower cone generator (windward side), obtained numerically and experimentally. As can be seen on the graph, the Simeonides criterion in this case gives a result very close to the experiment. In the color pictures of Fig. 8 LTT on the lower surface is seen as an area where the color changes from blue to red.

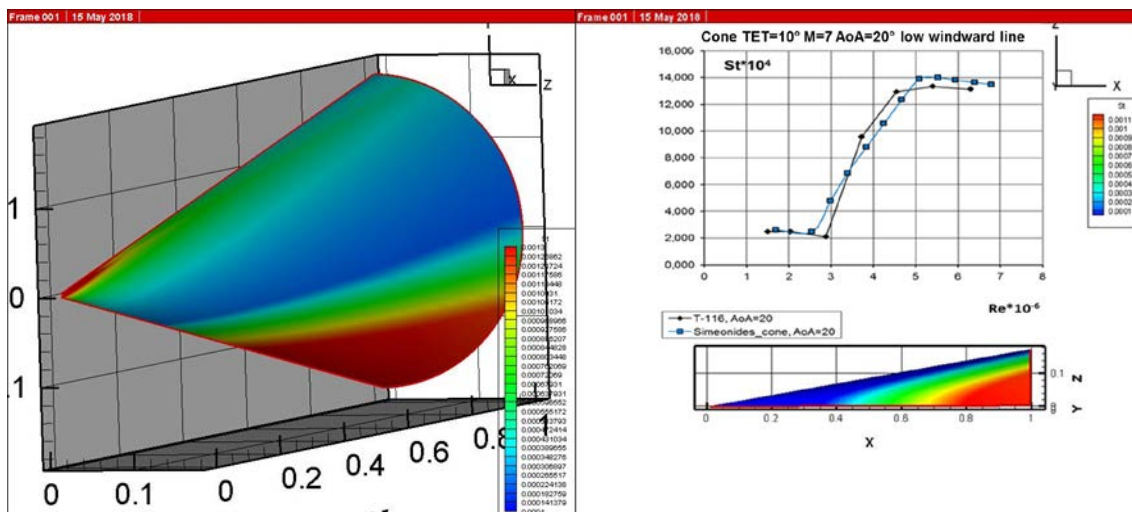


Fig. 8 The Stanton number on the surface of the cone, a comparison of experimental results and empirical criteria.

In Fig. 9 shows the distributions of the Stanton number along the lower cone generator with $\theta = 10^\circ$ at $M = 7$ and $\alpha = 0, 10^\circ, 20^\circ$ and 30° , obtained using a numerical method with the Simeonides criteria (left graph) and Berry (right graph). As can be seen from the presented graphs, the Simeonides criterion gives results closer to the experiment than the Berry criterion for most of the considered regimes. However, it is not right to conclude definitely that the Simeonides criterion always works better than the Berry criterion. In some modes, especially for the plate, the Berry criterion seems to be better. Therefore, in the future it seems appropriate to develop some combined criteria that will combine the merits of different empirical criteria.

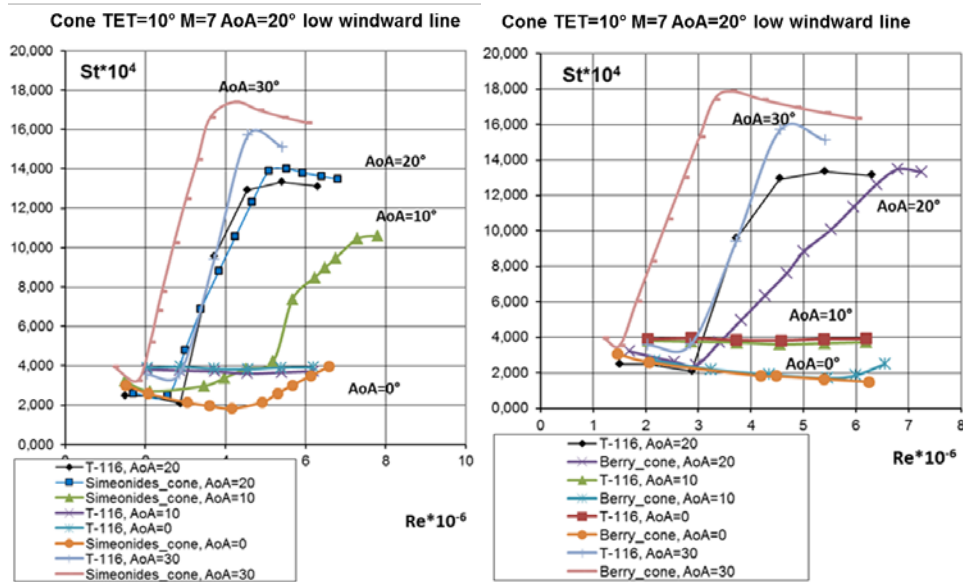


Fig. 9 The Stanton number on the surface of the cone, a comparison of experimental results and empirical criteria.

A comparison of the results of LTT simulations on the cone surface $\theta = 10^\circ$ at $M = 7$ and $\alpha = 20^\circ$ using a numerical-empirical method with the Simeonides and Berry criteria is shown in Fig. 10. As can be seen in the presented pictures and graphs, the Berry criterion gives a later onset of LTT and a longer transition zone than the Simeonides criterion. A similar picture is observed in most cases in the range of parameters under consideration.

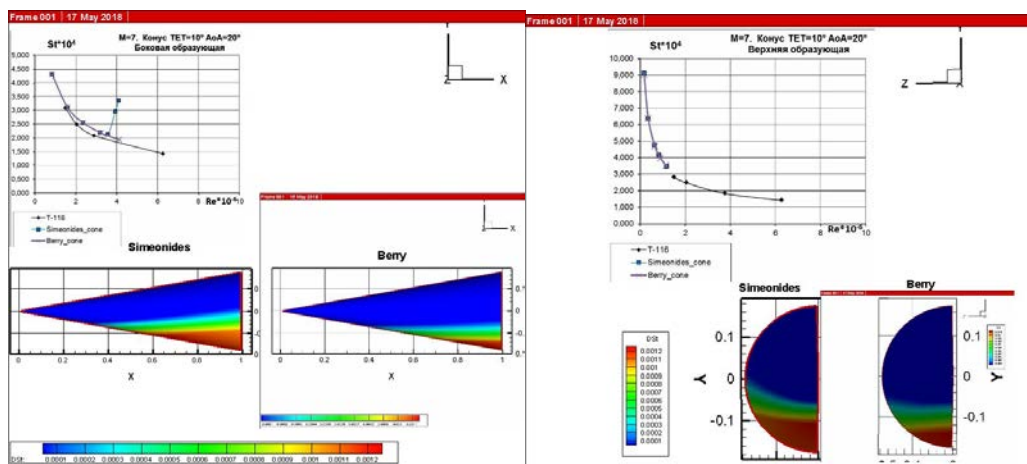


Fig. 10 LTT on the cone surface, comparison of the results of the empirical criteria of Simeonides and Berry.

As an example of a complex aerodynamic form on which the possibilities of numerically-empirical and CFD methods were investigated from the point of view of modeling flows with LTT, the glider model HEXAFly-INT was chosen. A detailed description of this model and previous LTT studies carried out within the framework of the international HEXAFly-INT project are described in [8]. Fig. 11 shows the results of LTT studies on the HEXAFly-INT model at $M_\infty = 7$, $\alpha = 0$. The presented figure summarizes

the results obtained by all three methods: the numerical-empirical method with the Simeonides criterion, a CFD with the Lentry-Menter LTT turbulence model, and wind-tunnel experiment in T-116 TsAGI. The presented results demonstrate a fairly good agreement, especially taking into account the geometry complexity.

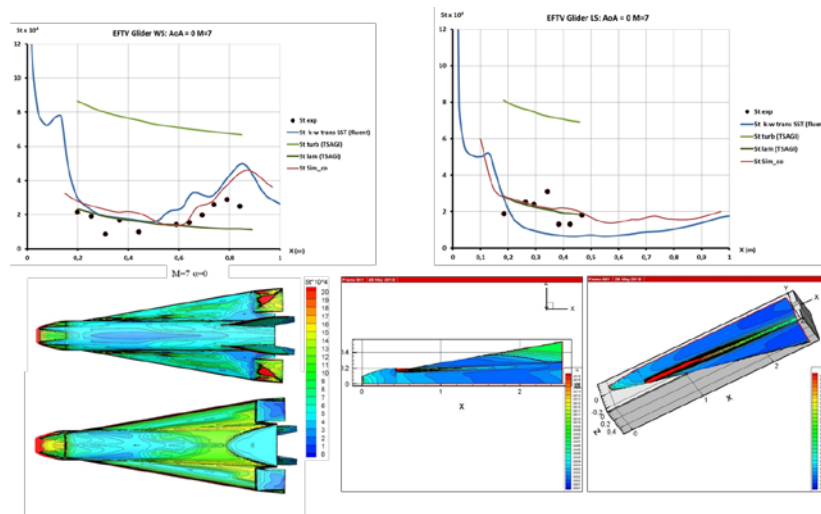


Fig. 11 LTT on the surface of HEXAFly-INT model.

A characteristic feature of the flow on the upper (leeward) side of this model is the formation of powerful vortex structures that descend from the nose leading edges and propagate downstream, affecting the surface of the wing and fuselage. Such structures are clearly visible in the left-hand pictures of Fig. 12, which show the fields of Mach numbers and current lines. These vortices initiate LTT on the surfaces in the area of the wing-fuselage joint, which is seen as the red areas in turbulence intensity images (central images) and Stanton numbers (right-hand pictures). The left and center images are obtained with the ANSYS FLUENT package, the right ones using the numerically-empirical method with the Simeonides criterion. It can be seen that the pictures of LTT, obtained by different methods, qualitatively coincide. With the growth of the angle of attack (the lower row of pictures), the vortex coming from the nose edge moves up and ceases to affect the upper surface of the aircraft, as a result of which the majority of the leeward surface flows with the laminar BL, and downstream the flow is relaminarized. This is also seen in the pictures of the lower row, obtained by different methods.

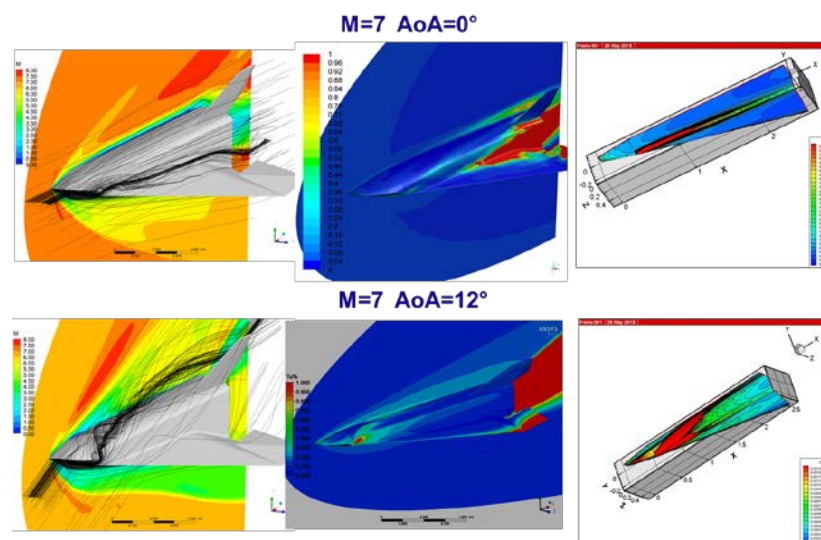


Fig. 12 LTT on the surface of HEXAFly-INT model, $M_\infty=7$, $\alpha=0, 12^\circ$.

Numerical studies carried out in the framework of the RANS equations with transitional turbulence models and empirical criteria have shown quite good agreement between the results and experimental

data. This approach is not completely correct, but it allows, at least, obtaining qualitative approximate data, which, of course, requires verification and comparison with the experimental data.

Conclusions

A laminar-turbulent transition was studied on the models of rectangular wing, cones, and on the HEXAFly-INT glider model, based on:

- Numerical simulation with the ANSYS FLUENT package with the SST transition turbulence model, which allows modeling of LTT;
- The numerical-empirical method, using the empirical criteria of Simeonides and Berry to estimate the transition onset and the transition region length;
- Experimental studies in TsAGI's wind tunnel T-116.

The results of different research methods are in qualitative agreement. It is impossible to determine unequivocally which of the empirical criteria is best, since the Berry criterion works better in the case of a straight wing (plate), and the Simeonides criterion gives results closer to the experiment on cones.

In most of the considered modes, the LTT on the windward side of the HEXAFly-INT model starts approximately at the middle of the model length and ends after its termination. On the leeward side of the model, in most cases the flow is laminar. A significant influence on the flow pattern on the leeward side of the model is provided by complex vortex structures coming off the edges of the nose and wing. They initiate transient phenomena downstream. In general, the flow past the HEXAFly-INT glider model is a mixed laminar-turbulent one, therefore, in the considered flow regimes of similar models, it is necessary to use computational methods with LTT simulation.

References

1. Воеводенко Н.В. Возможности расчета обтекания летательных аппаратов сложных форм при больших сверхзвуковых числах Маха с использованием гиперзвуковой теории малых возмущений. Журнал «Ученые записки ЦАГИ», 1988, том XIX, № 6.
2. N.V. Voevodenko Computation of Supersonic/Hypersonic Flow Near Complex Configurations. ICAS-94-5.2.3 (19th ICAS Congress, Anahime, CA, USA) Shvaley Yu.G.: Experimental investigation of the local heat transfer in laminar boundary layer at supersonic velocities. TsAGI scientific notes, Vol. IX, № 5, (1978)
3. Ragulin N.F. and Shvaley Yu.G.: Experimental investigation of the local heat transfer in turbulent boundary layer at supersonic velocities. Journal of Engineering and Physics, Vol. XLV, №4, (1983)
4. Simeonides G.A.: Laminar-Turbulent Transition Correlations in Supersonic/Hypersonic Flat Plate Flow – Attached versus Separated Flow. 26th International Congress of the Aeronautical Sciences, 14 - 19 September 2008, Anchorage, Alaska, USA (2008) Hamburger, C.: Quasimonotonicity, regularity and duality for nonlinear systems of partial differential equations. Ann. Mat. Pura Appl. 169, 321–354 (1995)
5. Berry S. et al.: Boundary Layer Transition on X-43A', 38th AIAA Fluid Dynamics Conference. Seattle WA, USA, 23-26 June 2008: AIAA-2008-3736 (2008)
6. F.R. Menter, R.B. Langtry. 2009. Correlation-Based Transition Modeling for Unstructured Parallelized Computational Fluid Dynamics Codes. AIAA J. 47(12), 2984-2906/
7. Voevodenko N.V., Gubanov A.A., Ivanyushkin D.S., Shvaley Y.G., Steelant J.: CFD and Experimental Simulation of the Laminar-Turbulent Transition on the HEXAFly-INT Glider Model. 7th European Conference for Aeronautics and Space Sciences (EUCASS), Milan, Italy, 3-6 July 2017: ID 419 (2017)
8. Kondratiev G.M. 1954. Regular heating regime. In: *Technical theoretical literature edition*.
9. Ю.Г. Швалеv Исследования перехода ламинарного пограничного слоя в турбулентный на моделях в аэродинамической трубе Т-116 ЦАГИ // Труды ЦАГИ, 2011, Выпуск 2693, (2011)